Development of Nano-Structured Hemocompatible Surfaces

Anthony J. Schrauth, Nannaji Saka, and Nam P. Suh
Deptartment of Mechanical Engineering, Massachusetts Institute of Technology
77 Massachusetts Avenue, Cambridge, MA 02139-4307, USA e-mail:(schrauth, nsaka, npsuh)@mit.edu

Abstract—**Hemocompatible surfaces are crucial to the performance of many biomedical devices. One of the requirements for such surfaces is the ability to resist the build-up of proteins from blood. We have been investigating the use of surface topography to minimize fluid-surface interaction with the goal that this phenomenon can then be exploited to decrease protein deposition on biomedical surfaces. This paper presents theoretical backing for the effect of surface structure on fluid wetting. We demonstrate the ability to control fluid-surface interaction by modifying surface structure. In one experiment, the apparent contact angle of a surface has been changed from 100° (flat surface) to 160° (structured surface). We present several alternative methods of creating micro-structure over a large area. We also show progress towards a method to manufacture nano-scale surface strutures over a large area.**

I. Introduction

Hemocompatibility is a major issue in biomedical systems design. Materials used for these devices must not interact unfavorably with blood. One major aspect of hemocompatibility is the ability of a surface to resist the deposition of proteins from the blood onto the surface. Protein deposition triggers clotting and can cause the device to function improperly or fail outright. This is unacceptable in biomedical applications where device robustness is paramount. Current biomedical surfaces use chemical and biological means such as specially designed coatings to resist protein deposition. Despite extensive effort, hemocompatibility remains an issue in biomedical systems.

We propose to improve hemocompatibility by modifying surface structure at the nano-scale to reduce blood clotting on artificial surfaces. This nanostructure will minimize the actual contact area between the blood and the surface and therefore slow the rate at which blood proteins coagulate on the surface. This approach can be used in conjunction with current hemocompatible materials to extend the life of biomedical implants, to decrease the cleaning required for external blood-handling equipment, and to increase the accuracy of blood testing devices.

The ultimate objective of this research is a commercially feasible method to manufacture nano-structured biocompatible surfaces. These surfaces will be applied to biomedical devices to reduce protein coagulation.

So far, our research has focused primarily on the development of feasible techniques to manufacture nano-structured surfaces rather than hemocompatible surfaces specifically. We are in the process of developing the appropriate testing methods and securing university approval to run experiments with biological materials. Consequently, this paper will focus only on fluid behavior and surface manufacturing with the goal of extending the investigation to bio-chemical behavior in the near future.

II. Background

Fluid wetting of a surface is generally described by Young's equation:

$$\cos(\theta) = \frac{\gamma_{SV} - \gamma_{SL}}{\gamma_{LV}}, \quad (1)$$

where γ_{SV}, γ_{SL}, and γ_{LV} are surface energies (solid/vapor, solid/liquid, and liquid/vapor, respectively) and θ is the contact angle between the liquid and the solid surface. Low contact angles (below 90°) indicate wetting of the solid by the fluid, with a contact angle of zero being complete wetting. High contact angles (above 90°) indicate non-wetting behavior, with a contact angle of 180° being complete non-wetting. Young's equation suggests that the contact angle can only be modified by controlling surface chemistry (i.e., changing the surface energies of the materials involved). Young's equation, however, is only valid macroscopically for flat and homogenous surfaces. Consequently, if we are only interested in macroscopic or apparent contact angles, then we have another method with which to control contact angles: surface structure.

Not unexpectedly, nature has already developed this solution. In 1990 Wilhelm Barthlott [1,2] discovered that the lotus plant (*Nelumbo nucifera*) used small bumps on the leaf surface to provide its famed resistance to fouling. Any debris that found its way onto the leaf could only contact the surface at the peaks of the bumps. Similarly, a water droplet rolling down the leaf would also only touch the tops of the bumps. When the droplet rolls over the debris, there is a much larger contact area between the debris and the water than between the debris and the leaf. Hence, there is a larger energy penalty for the debris particle to separate from the droplet than to separate from the surface peaks. Consequently, the debris sticks to the droplet as it rolls off the leaf. Barthlott dubbed this behavior "The Lotus Effect." Since his discovery, "The Lotus-Effect" has been extended to several commercial applications including self-cleaning automotive paint [3], waterproofing sprays, and others.

Even before Barthott's discovery, structured surfaces were used to modify solid-solid surface. In the 1980s low-friction surfaces [4], low-wear surfaces [4], and improved electrical connectors [5,6] were created using undulating surfaces.

III. Theory

Despite the recent euphoria of the "Lotus-Effect," interest in surface non-wetting by surface structuring is not a new idea. In the 1930s and 1940s the textile industry studied the phenomenon with the intent to design waterproof fab-

rics. From that research emerged two main theories relating surface structure to apparent contact angle. The first theory was proposed by Wenzel [7,8] and assumes that the fluid completely wets the solid structure (Fig. 1a). The second theory, presented by Cassie and Baxter [9], assumes that the fluid does not wet the valleys of the structure, but instead sits atop the peaks only (Fig. 1b). In both cases, the surface is assumed to be homogenous and the feature size is assumed to be much smaller than the apparent contact area.

Under Wenzel's assumption, the actual solid-liquid contact area is greater than the apparent (flat, smooth surface) contact area. Wenzel defines a roughness factor, *r*, as the ratio of the true contact area to the apparent contact area. The free energy of the liquid-solid interface on a rough surface is then *r* times greater than the free energy of a perfectly smooth surface with the same apparent contact area. Young's Equation, therefore, becomes

$$\cos\theta^* = \frac{r(\gamma_{SV} - \gamma_{SL})}{\gamma_{LV}} = r\cos\theta, \quad (2)$$

where θ^* is the apparent contact angle. We can see that an increase in roughness will increase θ^* for $\theta > 90^\circ$ and will decrease θ^* for $\theta < 90^\circ$. It is impossible for the apparent contact angle to be greater than 180° ($\cos\theta^* = -1$) or less than 0° ($\cos\theta^* = 1$), which can occur according to this equation if *r* becomes sufficiently large. Wenzel does not address this scenario. It is clear, however, that as the apparent contact angle approaches 180° the contact area between the fluid and the solid becomes small; this eventually violates one of the assumptions of Wenzel's theory, that the contact area is large compared with the surface features. Consequently, $\cos\theta^*$ most likely approaches ±1 asymptotically, though this case has not been investigated.

Under the Cassie-Baxter assumption, the fluid forms a composite surface with the solid, alternating between a fluid-solid interface and a fluid-vapor interface. If we define ϕ_S to be the area fraction of fluid-solid interfaces compared to the total apparent contact area, then the surface free energy created by a unit increase in the apparent contact area is:

$$\phi_S(\gamma_{SV} - \gamma_{SL}) - (1 - \phi_S)\gamma_{LV}. \quad (3)$$

If we substitute this expression into Young's equation in place of its equivalent for a homogenous surface, $(\gamma_{SV} - \gamma_{SL})$, then the equation for the apparent contact angle becomes:

$$\cos\theta^* = \frac{\phi_S(\gamma_{SV} - \gamma_{SL})}{\gamma_{LV}} - (1 - \phi_S). \quad (4)$$

Substituting Young's equation back into this expression gives the Cassie-Baxter equation for the apparent contact angle of a structured surface:

$$\cos\theta^* = \phi_S(\cos\theta + 1) - 1. \quad (5)$$

For materials with $\theta > 90^\circ$ a decrease in ϕ_S will increase the apparent contact angle. For surfaces with $\theta < 90^\circ$, however, the composite wetting assumption on which the theory is based, cannot hold because the capillary forces tend to drive the fluid into the valleys.

Both theories appear to be valid, and both are supported by independent investigations [10-14]. The wetting condition (composite or complete) is the determining factor for which theory applies to a specific case. To determine the particular wetting condition, we decided to investigate a simplified two-dimensional system (Fig. 2). Assuming that the fluid approaches the solid from above the surface structure (as opposed to being injected from the bottom), then the first condition that is physically reached in the composite wetting condition. If the fluid can be supported in this condition, then the Cassie-Baxter Theory applies, if not, the Wenzel Theory applies.

In order to determine the conditions under which the fluid will stay atop the features, we developed simple model. We assume vertical features as shown in Fig. 2, neglect gravity, and apply Laplace's equation for surface curvature,

$$\Delta P = \gamma_{LV}\left(1/R_1 + 1/R_2\right), \quad (6)$$

where R_1 and R_2 are the principal radii of curvature and ΔP is the pressure difference across the surface. If we assume one-dimensional (1-D) curvature ($R_2=\infty$), a given fluid pressure (ΔP) we can find the radius of the fluid surface curvature (R_1). From geometry we see that a given surface curvature and feature spacing will uniquely determine a contact angle (θ) between the liquid and the vertical wall of the feature. If this angle is less than the contact angle of the fluid with a flat surface of the same material, then the fluid will not descend into the grooves. Therefore, it is possible to define a critical feature spacing that will support a given fluid pressure without wetting the grooves.

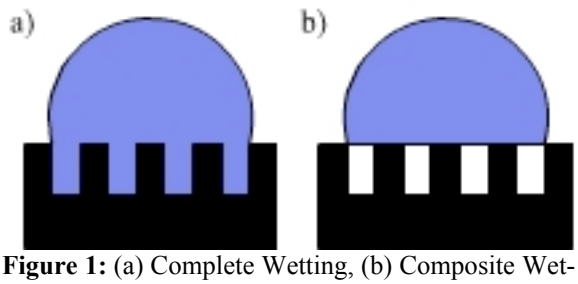

Figure 1: (a) Complete Wetting, (b) Composite Wetting.

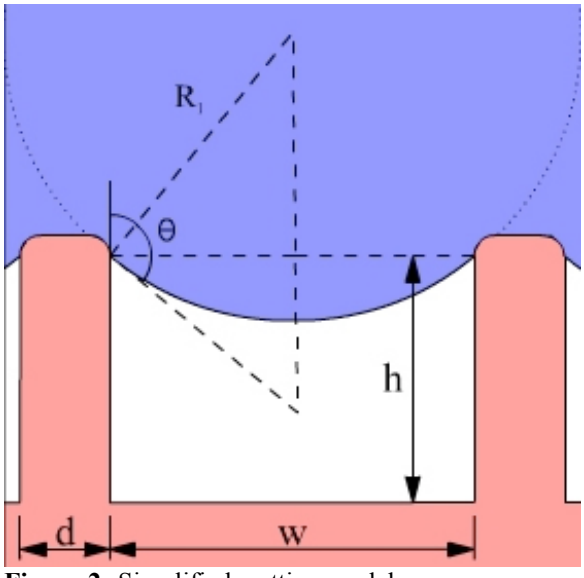

Figure 2: Simplified wetting model.

This analysis can be extended to the 2-D curvature case with more complicated geometry; the key result—that decreasing feature spacing increases the total pressure that the structure can support—will, however, remain the same.

IV. Axiomatic Design of a Non-wetting Surface

In order to develop appropriate surface structures we apply the Axiomatic Design theory [15]. The top-level functional requirement (FR_1) is to increase the apparent contact angle between the fluid and the surface. This requirement is satisfied by an appropriately chosen surface structure, which is the top-level design parameter (DP_1). FR_1 decomposes to FR_{11}: Reduce Wetting, and FR_{12}: Support a specified minimum fluid pressure (ΔP). These FRs are satisfied by DP_{11}: Surface structure with low area fraction (ϕ_S) and DP_{12}: Sufficiently small feature spacing. We know from the Cassie-Baxter theory that ϕ_S (DP_{11}) corresponds directly to a reduction in wetting (FR_{11}). Our wetting model shows that the correct feature spacing (DP_{12}) will specify the pressure that a structure can support (FR_{12}). This results in an uncoupled design as shown in the design equation:

$$\begin{Bmatrix} FR_{11} \\ FR_{12} \end{Bmatrix} = \begin{bmatrix} X & 0 \\ 0 & X \end{bmatrix} \begin{Bmatrix} DP_{11} \\ DP_{12} \end{Bmatrix}. \quad (7)$$

In addition to the FRs we have several constraints (Cs) on the design that must be satisfied. The first constraint (C_1) is that the surface material must start with a flat-surface contact angle greater than 90˚. Both the Cassie-Baxter and Wenzel theories indicate that contact angle can only be pushed away from 90˚ by the introduction of surface structure, so if we want to increase the contact angle, then the material must be at least slightly hydrophobic. Additionally, the fluid must not be able to wet the valleys of the structure. This means that when the fluid sits atop the post, the meniscus between the features must not touch the bottom of the valleys. This leads to a second constraint (C_2) that the aspect ratio (h/w) of the valleys must be much greater than a specific value that is dependent on the material's flat-surface contact angle. Assuming that the fluid forms a semi-cylindrical meniscus (Fig. 2), the minimum aspect ratio (AR_{min}) is:

$$AR_{\min} = \frac{1-\sin\theta}{-2\cos\theta}. \quad (8)$$

This constraint provides an acceptable range for the final free surface structure parameter, feature height. Additionally, we want this surface to be applicable on an 'engineering scale' so a third constraint (C_3) is that the structured surface must have an area much greater than, say, $10cm^2$.

V. Materials and Methods

For the purposes of investigating the fluid behavior on a surface we used deionized water exclusively. We did some blood tests to ensure that blood, as a fluid, behaves similarly to water. It turns out that the contact angle of blood on a surface was within a degree or two of the contact angle for water on the same surface. All contact angles were measured using a horizontally mounted microscope viewing a 5-µl sessile drop of water. The apparent contact angle was measured by hand using a protractor on the microscope images.

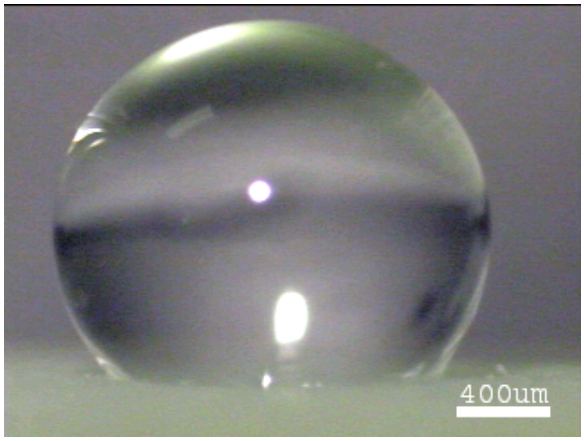

Figure 3: 5-µl water droplet on a tulip leaf.

VI. Experiments and Results

Our first step in this investigation was to test biological surfaces said to exhibit the "Lotus-Effect." One such example is the leaf of a tulip. The tulip leaf has a contact angle of 130˚ as shown in Fig. 3. The 5-µl drops do not roll off the leaf when it is tilted, but slightly larger drops roll extremely quickly without leaving a noticeable trail. The tulip leaf achieves its hydrophobic behavior with a tangled array of micro-scale hairs on the leaf surface (Fig. 4).

With an understanding of how the biological surface behaved, we moved on to determining how to create an artificial surface with similar behavior. The first step was to determine an appropriate material. Based on our first constraint, we needed a hydrophobic material. We settled on an elastomer, Poly(Dimethylsiloxane) (PDMS) (Sylgard 184, Dow-Corning, Midland, MI), that is popular for use in microfluidics and bioMEMS. It is both hydrophobic (θ_C=107˚) and biocompatible. Additionally, casting PDMS does not require extreme temperatures or a long cure time.

The first surface we cast in the PDMS was a monofilament nylon woven fabric. The fibers have a diameter of 35µm and are woven such that the fabric has 35µm square holes each separated by one 35µm diameter fiber. The

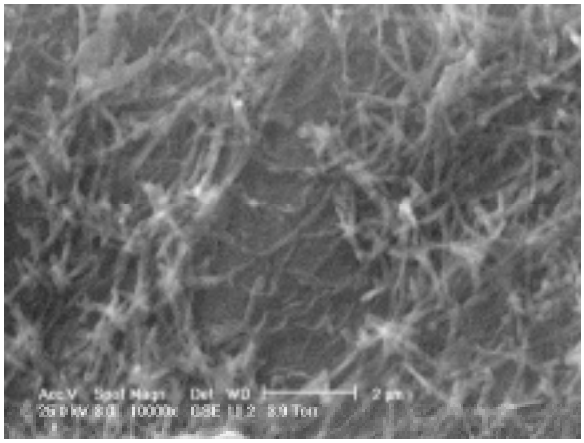
Figure 4: Environmental SEM image of a tulip leaf.

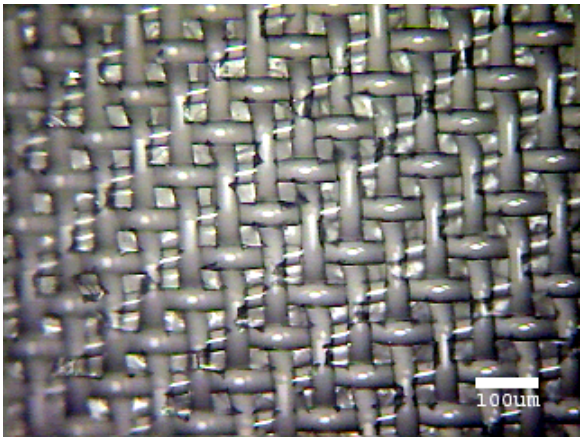

Figure 5: PDMS cast on nylon mesh.

PDMS cast on the nylon cloth is shown in Fig. 5. The PDMS penetrated the pores in the fabric and spread out on the backside. When the PDMS was removed from the fabric, some sections of cured PDMS from the backside of the fabric came through the holes resulting in some of the posts having "T" tops. The end result is a surface structure with an area ratio (ϕ_s) slightly larger than 0.25. According to the Cassie-Baxter Theory, ϕ_s=0.25 should yield an apparent contact angle of 145˚. Our cast had an apparent contact angle of 135˚ (Fig. 6), This difference is most likely caused by the "T"-topped features and the fluid slightly descending the features. Both of these factors would increase ϕ_s and thus decrease the apparent contact angle.

In the interest of reducing the surface area fraction, we tried a 1-D array of features similar to the nylon weave. We tightly wrapped a piece of nylon fishing line (300-µm diameter) around a frame to form a 1-D array of semi-circles onto which we cast PDMS. The resulting surface (Fig. 7) had 30µm wide peaks separated by 300-µm wide semi-circular valleys. This surface exhibited a maximum apparent contact angle (looking parallel to the lines) of 150˚ (Fig. 8) but the apparent contact angle (looking parallel to the lines) also varied greatly between 125˚ and 150˚. It was clear that when the water stayed on top of the features, the contact angle was large and once the water descended into the features, the contact angle dropped drastically. The area ratio for this surface was excellent (ϕ_s=0.09), but the

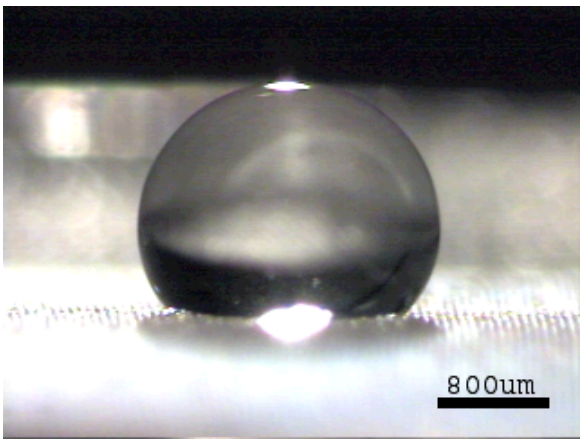

Figure 6: 5-µl water droplet on a PDMS cast of nylon mesh.

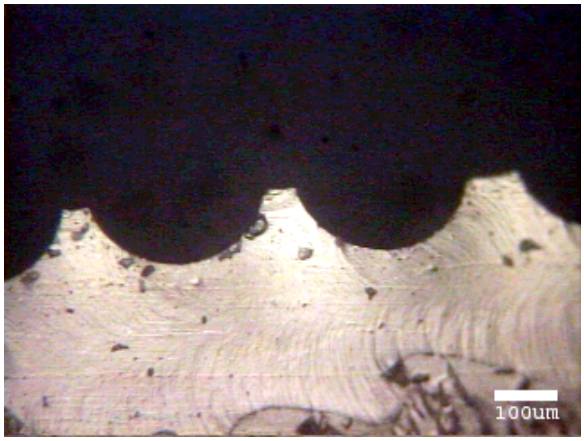

Figure 7: PDMS cast on nylon fishing line.

feature spacing was too large to support a droplet of water.

In order to reduce the feature spacing while keeping the low area ratio, we tried using thin copper wire (80-µm diameter) instead of nylon fishing line. The resulting surface did have a similar area ratio to the nylon version, but it was not as consistent. There were areas where the several features are joined together into one large feature. Even so, the surface has an apparent contact angle (looking parallel to the lines) of 150˚ (Fig. 9) that was much more robust than the large-scale surface with a similar area ratio.

It is important to note that neither the Wenzel theory or the Cassie-Baxter theory apply directly to 1-D arrays of features because the structure is large compared with the contact area and is not homogenous; thus this case violates the basic assumptions of both theories. It is clear, however, that the idea of reducing area ratio or increasing roughness, even in only one direction, to increase apparent contact angle still holds. Not surprisingly, the resulting sessile drop in this case was not axisymmetric but rather elongated in the direction of the lines.

The above experiments offered confidence in the theories from which we are designing our features, but we needed to have more controlled tests. For this employed photolithography. We used masks patterned with 20µm square posts with area ratios (ϕ_s) equal to 0.04, 0.08, 0.12, or 0.16. The patterns were transferred to 45µm thick SU-8 2100 photoresist (Microchem, Newton, MA) via photolithography (Fig.

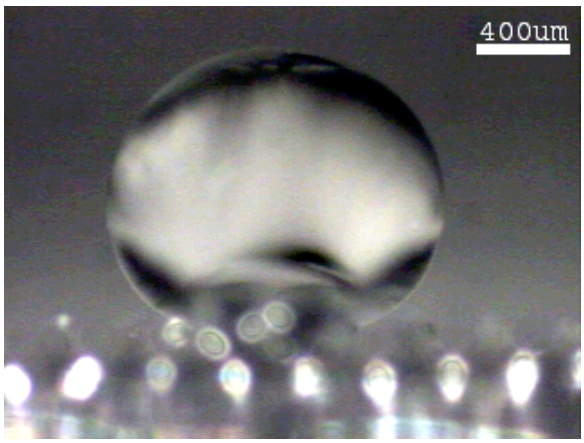

Figure 8: 5-µl water droplet on a PDMS cast of nylon fishing line.

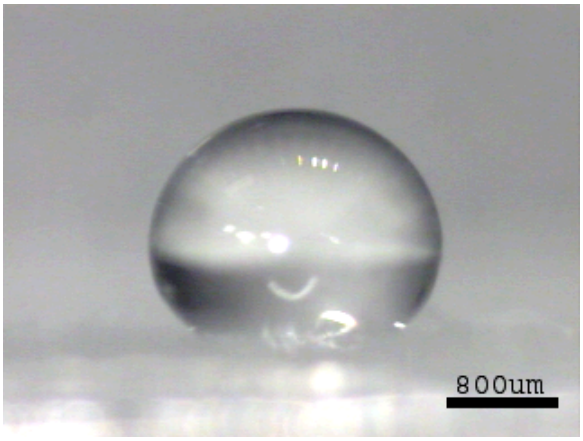

Figure 9: 5-µl water droplet on a PDMS cast of copper wire.

10). For our biological experiments, we will cast these surfaces twice in PDMS to get the positive image of the features in PDMS [16]. In the interest of simplicity, we coated the patterns in (Tridecafluoro-1,1,2,2-tetrahydrooctyl)Tricholorosilane (Gelest Inc., Morrisville, PA) to make them hydrophobic. The contact angle of the silane is 100˚ on a flat surface. The apparent contact angles for the structured surfaces were 160˚, 150˚, 145˚, and 130˚ for mask area ratio (ϕ_s) equal to 0.04, 0.08, 0.12, and 0.16 respectively. The actual area ratios of the SU-8 structures were slightly larger than the intended area ratios due to inaccuracies in the pattern transfer. Using the actual area ratios of the surfaces, the predicted apparent contact angles for the four surfaces (ϕ_s =0.04-0.16) were 162˚, 154˚, 149˚, and 142˚. Fig. 11 shows a droplet on a flat surface next to a droplet on the SU-8 pattern with (ϕ_s=0.04).

The SU-8 surfaces offer excellent geometry control, but photolithography and similar techniques used for nanofabrication are severely limited by their expense and their area of effect. Consequently, we are interested in methods that can be applied to larger areas. One option we came up with was to use nano-porous aluminum oxide as a mold for PDMS. When aluminum is oxidized in certain electrolytes (sulfuric, oxalic, and phosphoric acid) it self-assembles into pores arranged in a honeycomb pattern [17-21]. The pore structure is uniform enough so that aluminum oxide can be used to make high-quality particulate filters. Fig. 12

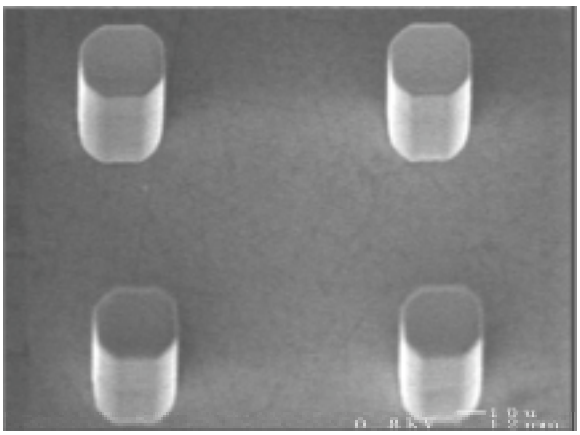

Figure 10: SEM image of SU-8 structure (ϕ_s=0.04) viewed 30¢™from normal.

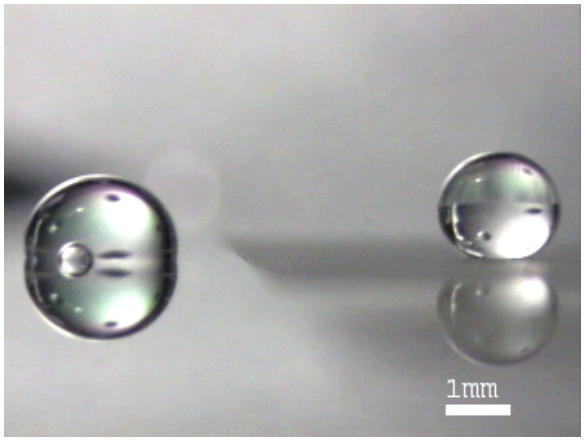

Figure 11: 5-µl water droplets on a flat surface (left) and on a SU-8 structured Surface with ϕ_s=0.04 (right).

shows an SEM image of one of these filters with a 200nm pore size. The walls between pores are approximately 25nm thick. According to the Cassie-Baxter theory, a cast of this pattern will only yield a contact angle of 115˚. Even so, the prospect of being able to structure any surface that can be made out of aluminum makes it worthwhile to investigate.

Unfortunately, casting PDMS off of the aluminum oxide filters is extremely difficult. The uncured PDMS penetrates the filter pores but it is exceedingly difficult to remove the PDMS once it has been cured. The filters are extremely brittle and tend to break when we attempt to separate the PDMS from the aluminum oxide mold. To eliminate the problem of mold fracture, we anodized aluminum and left the aluminum oxide layer on the base material. Using sulfuric acid as an electrolyte, we were able to create 25nm pores in aluminum oxide (Fig. 13). The PDMS separated easily from the aluminum oxide left on the base aluminum, but the features did not transfer to the PDMS. Since the features in the aluminum oxide are only 25nm we do not need very tall features to satisfy the aspect ratio constraint. Any extra height is only making it more difficult to remove the PDMS and keep the features intact. If we can reduce the depth that the PDMS penetrates the aluminum oxide, then we may be able to remove the PDMS more easily. We are currently investigating ways to control the size and spacing of the pores and ways to limit PDMS penetration.

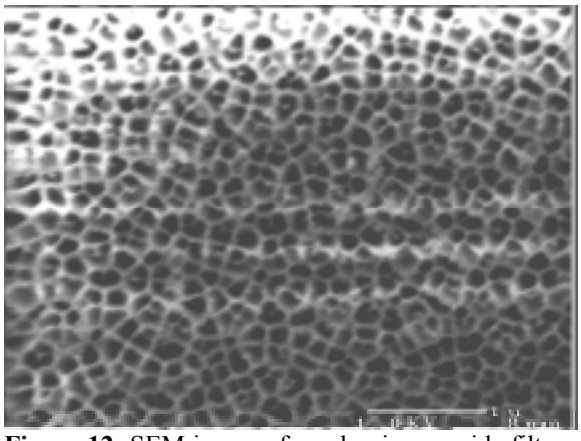

Figure 12: SEM image of an aluminum oxide filter.

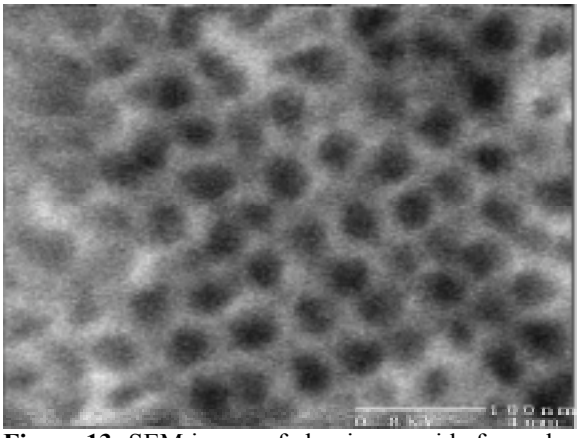

Figure 13: SEM image of aluminum oxide formed by anodizing in sulfuric acid.

VII. CONCULSIONS

Surface topography is a powerful method for modifying the wetting characteristics of a fluid-surface interface. We have demonstrated that even surface features on the micron scale can dramatically change a surface's apparent contact angle. Nano-scale features offer more robust control of wetting behavior, but current nano-fabrication techniques are not appropriate for structuring large area surfaces; the improvement in surface functionality they offer does not justify the cost and time required for current techniques. Consequently, we are working towards a method that will allow us to apply a nano-structure over a very large area surface.

In addition to developing new surface manufacturing techniques, we will be testing the ability of our structured surfaces to reduce blood protein coagulation. Presumably, blood proteins will behave in a similar fashion to the debris on a lotus leaf in that a reduction in the available contact area will reduce the ability of the protein to stick to the surface. Nano-structuring may also offer additional functionality over micro-structuring in this respect. The cells and molecules with which we are concerned have sizes on the order of microns. Thus, these cells would not be able to fit into the surface features of a nano-structured surface. This may further improve the hemocompatibility of the structured surfaces.

VIII. ACKNOWLEDGEMENTS

We would like to thank Dr. San-Rok Lee, director of the Center for Nanoscale Mechatronics and Manufacturing (CNNM), for his support of the "21st Century Frontier Program in Nanoscale Mechatronics and Manufacturing" at MIT. We are also indebted to Professor Jung-Hoon Chun for his contributions to this work. Additionally, we would like to thank the Korea Institute of Machinery and Materials (KIMM) and CNNM for their support of this research.

IX. REFERENCES

[1] W. Barthlott, *Scanning electron microscopy in taxonomy and functional morphology*, D. Claugher, Oxford: Clarendon Press, 1990, 69–94.

[2] W. Barthlott and C. Neinhuis, "Purity of the sacred lotus, or escape from contamination in biological surfaces," *Planta*, 202, 1, April, 1997, 1-8.

[3] M. Wulf et al, "Coatings with Self Cleaning Properties," in *Quo Vadis-Coatings?: XXVI FATIPEC Congress*, 2002, 459-467.

[4] *Tribophysics*, N. P. Suh, Englewood Cliffs, NJ: 1986.

[5] N. P. Suh and M. Sweetland, U.S. Patent pending.

[6] N. Saka, M.J. Liou, and N.P. Suh, "The Role of Tribology in Electrical Contact Phenomena," *Wear,* 100, 1-3, December, 1984, 77-105.

[7] R. N. Wenzel, "Resistance of solid surfaces to wetting by water," *Industrial and Engineering Chemistry*, 28, 8, August, 1936, 988-994.

[8] R. N. Wenzel, "Surface Roughness and Contact Angle," *Journal of Physical Colloid Chemistry*, 53, 9, December, 1949, 1466-1467.

[9] A. B. D. Cassie and S. Baxter, "Wettability of Porous Surfaces," *S. Trans. Faraday Soc.*, 40, 1944, 546-551.

[10] T. N. Krupenkin et al, "From Rolling Ball to Complete Wetting: The Dynamic Tuning of Liquids on Nanostructured Surfaces," *Langmuir*, 20, 10, May, 2004, 3824-3827.

[11] N. A. Patankar, "On the Modeling of Hydrophobic Contact Angles on Rough Surfaces," *Langmuir*, 19, 4, February, 2003, 1249-1253.

[12] J. Bico et al, "Pearl Drops," *Europhysics Letters*, 47, 2, July, 1999, 220-226.

[13] S. Shibuichi, "Super Water-Repellent Surfaces Resulting from Fractal Structure," *Journal of Physical Chemistry*, 100, 50, December,1996, 19512-19517.

[14] M. Miwa et al, "Effects of the Surface Roughness on Sliding Angles of Water Droplets on Superhydrophobic Surfaces," *Langmuir*, 16, 13, June, 2000, 5754-5760.

[15] *Axiomatic Design: Advances and Applications*, N. P. Suh, New York: 2001.

[16] J. L. Tan et al, "Cells lying on a bed of microneedles: An approach to isolate mechanical force," *Proceedings of the National Academy of Sciences of the United State of America*, 100, 4, February, 2004, 1484-1489.

[17] H. Masuda et al, "Self-Ordering of Cell Arrangement of Anodic Porous Alumina Formed in Sulfuric Acid Solution," *Journal of the Electrochemical Society*, 144, 5, May, 1997, L127-L130.

[18] A P. Li et al, "Hexagonal pore arrays with a 50-420 nm interpore distance formed by self-organization in anodic alumina," *Journal of Applied Physics*, 84, 11, December, 1998, 6023-6026.

[19] T. T. Xu et al, "Bone-Shaped Nanomaterials for Nanocomposite Applications," *Nano Letters*, 3, 8, August, 2003,1135-1139.

[20] H. Masuda and K Fukuda, "Ordered Nanohole Arrays Made by Two-Step Replication of Honeycomb Structures of Anodic Alumina," *Science*, 268, 5216, June, 1995, 1466-1468.

[21] O. Jessensky et al, "Self-organized formation of hexagonal pore arrays in anodic alumina," *Applied Physics Letters*, 72, 10, March, 1998, 1173-1175.